A push–pull mechanism for regulating integrin function

Wei Li*, Douglas G. Metcalf†, Roman Gorelik*, Renhao Li†‡, Neal Mitra*, Vikas Nanda†, Peter B. Law†, James D. Lear†, William F. DeGrado†§, and Joel S. Bennett*§

*Department of Medicine, Hematology–Oncology Division, and †Department of Biochemistry and Biophysics, School of Medicine, University of Pennsylvania, Philadelphia, PA 19104

Communicated by James A. Wells, Sunesis Pharmaceuticals, Inc., South San Francisco, CA, December 15, 2004 (received for review June 15, 2004)

Homomeric and heteromeric interactions between the αIIb and β3 transmembrane domains are involved in the regulation of integrin αIIbβ3 function. These domains appear to interact in the inactivated state but separate upon integrin activation. Moreover, homomeric interactions may increase the level of αIIbβ3 activity by competing for the heteromeric interaction that specifies the resting state. To test this model, a series of mutants were examined that had been shown previously to either enhance or disrupt the homomeric association of the αIIb transmembrane domain. One mutation that enhanced the dimerization of the αIIb transmembrane domain indeed induced constitutive αIIbβ3 activation. However, a series of mutations that disrupted homodimerization also led to αIIbβ3 activation. These results suggest that the homo- and heterodimerization motifs overlap in the αIIb transmembrane domain, and that mutations that disrupt the αIIb/β3 transmembrane domain heterodimer are sufficient to activate the integrin. The data also imply a mechanism for αIIbβ3 regulation in which the integrin can be shifted from its inactive to its active state by destabilizing an αIIb/β3 transmembrane domain heterodimer and by stabilizing the resulting αIIb and β3 transmembrane domain homodimers.

αIIbβ3 | integrin regulation | transmembrane domains

Integrins reside on cell surfaces in an equilibrium between inactive and active conformations that can be shifted in either direction by altering the distance between the stalks that anchor integrins in cell membranes (1). At the cellular level, integrin activation is regulated by cellular agonists, but how this occurs is uncertain. In the case of the platelet integrin αIIbβ3, membrane-proximal segments of the αIIb and β3 cytoplasmic (CYT) domains are thought to directly interact to constrain the integrin in an inactive state (2). Agonist-stimulated talin binding to the β3 CYT domain may relieve this constraint, inducing αIIbβ3 activation (3).

The αIIb and β3 transmembrane domains are also in proximity when the integrin is inactive and separate upon integrin activation (4). Moreover, these domains readily undergo homomeric interactions in micelles (5), and both homomeric and heteromeric interactions have been detected in biological membranes (6, 7). Thus, in the platelet membrane where the concentration of these domains is high, the αIIb and β3 helices might be expected to form homooligomers in the activated state, crosslinking individual molecules and stabilizing focal adhesions (8). Indeed, we tested this possibility previously by placing Asn, a residue known to strengthen homomeric transmembrane (TM) interactions (9, 10), at successive positions across a 10-residue segment of the β3 TM domain and found that mutations along one face of the helix led to constitutive αIIbβ3 activation and integrin clustering (11).

However, there are two distinct mechanisms by which TM domain mutations might activate integrins. Besides increasing the tendency of a highly expressed integrin to form homooligomers, TM domain mutations might disrupt heteromeric interactions and activate the integrin in this manner. Here, we examine mutants that either enhance or disrupt homooligomerization of the αIIb TM domain. Using the TOXCAT assay, we found previously that the sequence xxVGxxGGxxxLxx is critical for homooligomerization of the αIIb TM helix, and we identified mutations in the sequence that either increased or decreased the homomeric association of the αIIb TM helix (7). Thus, mutating either Gly in the strong homooligomerization motif GxxxG (12) to Ala, Leu, Val, or Ile decreased dimerization, whereas replacing the downstream Leu with Ala enhanced dimerization. Here, we have determined how these mutations, as well as Asn-scanning mutations of the αIIb TM helix, affect the αIIbβ3 activation state. Like oligomer-enhancing mutations in the β3 TM helix (11), we found that the homodimer-enhancing L980A mutation induced constitutive αIIbβ3 activity and clustering. However, we found that mutations that disrupted oligomerization also resulted in a constitutively activated phenotype, suggesting that these residues may be located at the interface between the αIIb and β3 TM domains. Together, these results suggest a push–pull mechanism for the regulation of the αIIbβ3 activity: events that disrupt the heterodimerization of the αIIb and β3 TM domains push the integrin toward the activated state, whereas events that enhance the homomeric association of these domains pull the equilibrium toward activation.

Materials and Methods

Stable Expression of αIIbβ3 Mutants in CHO Cells. Mutated αIIb and WT β3 cDNAs were subcloned into the plasmids pcDNA3.1(+)-Neo and pcDNA3.1(+)-Zeo, respectively, before cotransfection into CHO cells using FUGENE6 (Roche Diagnostics). Transfected cells were grown in a selection medium containing G418 and Zeocin for 3 wk before being sorted twice by FACS for cells expressing high levels of αIIbβ3 (11).

Fibrinogen Binding to CHO Cells Expressing αIIbβ3. CHO cells, at a density of 2×10^6 cell/ml, were incubated with the β3-specific mAb SSA6 (13) on ice for 30 min. The mAb-labeled cells were then washed and incubated for 30 min at 37°C with phycoerythrin (PE)-conjugated anti-mouse IgG (Molecular Probes) and 200 μg/ml FITC-conjugated fibrinogen. Freshly made 5 mM DTT and/or 5 mM EDTA were added to the incubations as indicated. After incubation, the cells were washed, fixed with 0.37% formalin in PBS, and examined by two-color FACS analysis, as described (14).

Immunostaining of αIIbβ3 on the CHO Cell Surface. αIIbβ3 clustering on the CHO cell surface was detected as described (11). Briefly, 4×10^6 CHO cells were fixed by using 4% paraformaldehyde before being transferred to a polylysine-coated chamber glass

Abbreviations: CYT, cytoplasmic; TM, transmembrane; PE, phycoerythrin; FAK, focal adhesion kinase; CAT, chloramphenicol acetyl transferase; GpA, glycophorin A.

‡Present address: Center for Membrane Biology and Department of Biochemistry and Molecular Biology, University of Texas Medical School, Houston, TX 77030.

§To whom correspondence may be addressed. E-mail: wdegrado@mail.med.upenn.edu or bennetts@mail.med.upenn.edu.

slide. The slides were then washed with 50 mM Tris·HCl, pH 7.4, blocked with 5 mg/ml BSA in PBS, and incubated sequentially with the anti-β3 mAb SSA6 and FITC-labeled anti-mouse IgG. Stained cells were mounted in Citifluor antifadant mounting material (University of Kent, Canterbury, U.K.) and examined by using a Nikon Microphot-SA fluorescence microscope. Images were captured by using IPLAB SPECTRUM IMAGE ANALYSIS software for the Macintosh and a Photometrics SenSys KF1400 camera (BioVision Technologies, Exton, PA). For each mutant, 30–40 stained cells were selected randomly and photographed.

Focal Adhesion Kinase (FAK) Phosphorylation. FAK phosphorylation in CHO cells adherent to fibrinogen-coated tissue culture plates or resuspended in centrifuge tubes was studied as described (15). Briefly, FAK was immunoprecipitated from 125 μg of total protein from lysed cells and subjected to SDS/PAGE in a 3–8% NuPAGE Tris-Acetate gel (Invitrogen). Anti-FAK polyclonal antibody (Upstate Biotechnology) was used for immunoprecipitation and immunoblotting. FAK phosphorylation was detected by using a mouse antiphosphotyrosine mAb (Upstate Biotechnology).

Expression and Purification of Proteins Corresponding to the TM/CYT Domains of αIIb and β3. Proteins corresponding to the TM/CYT domains of αIIb and β3 were expressed in *Escherichia coli* strain BL21 and purified by HPLC as described (5). Briefly, cDNAs corresponding to the αIIb and β3 TM/CYT domains were amplified by PCR by using αIIb and β3 cDNAs as templates, cloned into the vector pGEX-4T-3 (Amersham Pharmacia–Pharmacia), and expressed as glutatione *S*-transferase-fusion proteins. Synthesized fusion proteins were isolated by affinity chromatography by using glutathione-Sepharose 4B, the glutatione *S*-transferase was removed by cleavage with thrombin, and the cleaved samples were purified by preparative reverse-phase HPLC and lyophilized. The lyophilized proteins were then dispersed in dodecylphosphocholine dissolved in methanol and dried under a stream of nitrogen. The dried mixture was dissolved in aqueous buffer, and the protein concentration was determined by absorbance at 280 nm. The extinction coefficients for αIIb and β3 TM/CYT proteins were calculated as 16,500 $M^{-1}\cdot cm^{-1}$ and 13,980 $M^{-1}\cdot cm^{-1}$, respectively, based on the method by Pace *et al.* (16).

Analytical Ultracentrifugation. Equilibrium sedimentation was performed in a Beckman XL-I analytical ultracentrifuge (Beckman Coulter) at 25°C (5). D_2O was added to the buffer [10 mM dodecylphosphocholine (DPC)/20 mM 4-morpholinepropanesulfonic acid/100 mM KCl/1 mM $MgCl_2$, pH 7.4] to 50.34% to match the density of DPC. The molecular mass and partial specific volume of WT and mutant TM/CYT proteins were calculated and the data sets analyzed as described (5).

TOXCAT Assay. The TOXCAT assay (17) was performed by using the expression vectors pccKAN, pccgpA-wt, and pccgpA-G83I and the *E. coli* strain MM39 kindly provided by Donald M. Engelman (Yale University, New Haven, CT). After changing the *Eco*RV restriction site between the TM region and the malB gene in pccKAN to a *Bam*HI site, the vector was digested with *Nhe*I-*Bam*HI, and genes encoding the αIIb and β3 TM helices were ligated into the vector in-frame. Subsequent site-directed mutagenesis was performed by using a QuikChange mutagenesis kit (Stratagene). The resulting plasmids were transformed into *E. coli* MM39 cells. The optimal length of the αIIb TM helix for this assay was determined previously (7). To identify the optimal length for the β3 TM helix, we incrementally deleted residues from its C-terminal end. A helix encompassing residues 693–713 resulted in maximal chloramphenicol acetyl transferase (CAT) synthesis (data not shown) and was used in subsequent experiments.

CAT synthesis was assayed by using a CAT-ELISA kit (Roche Applied Sciences, Indianapolis), as described (7). In each experiment, glycophorin A (GpA)-WT was included for comparison. Results were expressed as a percentage of the CAT induced by GpA-WT in the same experiment. Chimeric protein expression was quantified from immunoblots by using a Personal Densitometer SI (Molecular Dynamics) and was used to compare CAT expression by the various constructs.

Table 1. Sequences of the αIIb and β3 TM domains

Domain	Sequence
αIIb 967–988	WW**VLVGVLGGLL**L**L**TI**L**VLAMW
β3 693–715	ILVVLLSVMGAILLI**G**LAALLIW

Sites mutated in the αIIb and β3 TM domains are shown in bold.

Structural Model of an αIIbβ3 TM Domain Heterodimer. An atomic model of an αIIb/β3 TM heterodimer was constructed by using a Monte Carlo simulated annealing algorithm (7). Two idealized helices corresponding to αIIb residues Ile-966 through Trp-988 and β3 residues Ile-693 through Trp-715 were docked by using six orthogonal parameters: three rigid body translations and three rotations. All canonical helical rotamers (18) were considered for residues along an interhelix interface; otherwise, the principal helical rotamer was selected. Side-chain conformations were selected by using dead-end elimination at each step of the process, and the energy of each structure was calculated by using the AMBER potential (19). At each step, the energies of both disruptive as well as silent mutations were evaluated for a given backbone geometry. The program maximizes the Boltzmann probability associated with the ensemble of silent mutations, while minimizing the Boltzmann probability of the ensemble of disruptive mutations. Energy minima were identified by using a simulated annealing algorithm with an exponential temperature decay (see supporting information, which is published on the PNAS web site).

Results

An Asn Substitution in the αIIb TM Domain Activates αIIbβ3. Addition of Asn to model TM helices promotes their association in biological membranes (9, 10). Previously, we demonstrated that substituting Asn for either of two appropriately spaced residues in the TM helix of β3 enabled αIIbβ3 to constitutively bind fibrinogen and enhanced the tendency of the helix to form homotrimers (11). As shown in Table 1, we placed Asn at 10 consecutive positions in the αIIb TM helix extending from residues V969 to L978 and coexpressed each mutant with WT β3 in CHO cells. We then measured the effect of the mutations on the ability of αIIbβ3 to bind fibrinogen constitutively and to form spontaneous αIIbβ3 clusters. Despite our previously reported results (11), the outcome of the current experiments was not predictable, because a single Asn can be a weaker signal for oligomerization than the preexisting strong dimerization GxxxG motif found in the αIIb TM domain (20, 21). Unless these two signals reinforce one another (22), it is possible that introducing Asn could disrupt the intrinsic tendency of the helix to dimerize.

We found the expression of αIIbβ3 containing 6 of the 10 Asn mutants on the CHO cell surface was comparable to that of αIIbβ3 containing WT αIIb (data not shown). However, the V971N, V973N, G976N, and L977N mutants were consistently expressed at substantially lower levels, suggesting their presence had a deleterious effect on αIIbβ3 biosynthesis.

We then used FACS analysis to measure the ability of WT αIIbβ3 and the highly expressed αIIb mutants to bind soluble fibrinogen, either constitutively or after αIIbβ3 activation using DTT. WT αIIbβ3, as well as each of the αIIb mutants, readily bound fibrinogen after exposure to DTT but only the G972N mutant bound fibrinogen constitutively. As shown in Fig. 1*A*, αIIbβ3 containing the G972N mutation bound ≈8-fold more

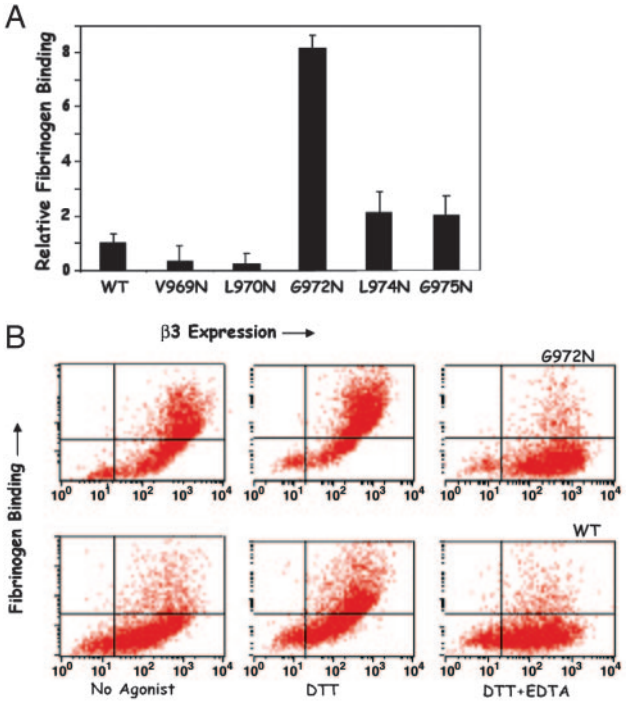

Fig. 1. Effect of Asn substitutions in the αIIb TM domain on αIIbβ3 function. (*A*) Constitutive fibrinogen binding to CHO cells expressing WT αIIbβ3 and various αIIb TM domain Asn mutants. Data are expressed as the ratio of cells constitutively binding fibrinogen to cells not binding fibrinogen determined from dot plots of two color FACS analysis and were normalized to data obtained from the cells expressing WT αIIbβ3. The data are the mean and SE of two to seven experiments. (*B*) Dot plots of fibrinogen and anti-β3 mouse mAb SSA6 binding to cells expressing WT human αIIbβ3 and the αIIb mutant G972N. FITC fluorescence, representing fibrinogen binding, is shown on the *y* axis, and PE fluorescence, representing β3 expression, is shown on the *x* axis. Fibrinogen binding was measured in the absence or presence of 5 mM DTT and in the presence of 5 mM EDTA.

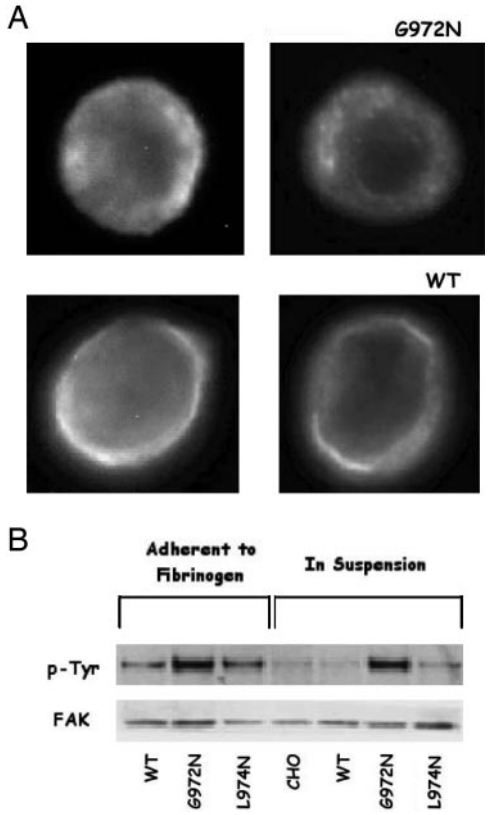

Fig. 2. The αIIb mutation G972N induces αIIbβ3 clustering. (*A*) Fluorescence microscopy of CHO cells expressing WT αIIbβ3 and the αIIb mutant G972N. Cells were fixed with paraformaldehyde, incubated sequentially with the mAb SSA6 and FITC-labeled anti-mouse IgG, and examined by fluorescence microscopy. Thirty to forty stained cells were randomly selected and photographed. Representative images are shown. (*B*) FAK phosphorylation in adherent and resuspended CHO cells expressing WT αIIbβ3 and the αIIb mutants G972N and L974N. (*Upper*) FAK phosphorylation detected by using an antiphosphotyrosine antibody. (*Lower*) FAK protein detected by using an anti-FAK antibody.

fibrinogen than did WT αIIbβ3 in the absence of DTT. Moreover, as illustrated by the histograms in Fig. 1*B*, ≈34% of the G972N cells expressed constitutively activated αIIbβ3, compared to only 3% of the WT cells. Nonetheless, both constitutive and DTT-induced fibrinogen binding was inhibited by the divalent cation chelator EDTA, consistent with specific fibrinogen binding to αIIbβ3 (11).

Activating αIIbβ3 by introducing Asn into the β3 TM helix resulted in αIIbβ3 clustering (11). To determine whether replacing G972 in the αIIb TM helix with Asn had the same effect, CHO cells expressing WT αIIbβ3 or the G972N mutant were fixed, stained sequentially with the β3-specific mAb SSA6 and FITC-labeled anti-mouse IgG, and examined by fluorescence microscopy. As shown in Fig. 2*A*, WT αIIbβ3 was present as a homogenous ring at the cell periphery. This ring was not present in cells expressing the G972N mutant; rather, αIIbβ3 was distributed in patches on the CHO cell surface, consistent with the presence of αIIbβ3 clusters.

αIIbβ3 clustering is accompanied by the autophosphorylation of FAK on tyrosine residues (23), as well as phosphorylation of FAK by activated Src kinases (24). To confirm that the fluorescent patches on cells expressing G972N resulted from αIIbβ3 clustering, we measured FAK phosphorylation in CHO cells expressing WT αIIbβ3 and the G972N and L974N mutants, both when the cells were adherent to fibrinogen and after they were placed in suspension (Fig. 2*B*). As expected, FAK was phosphorylated in adherent CHO cells expressing WT αIIbβ3 and those expressing either mutant, but little or no phosphorylation remained after cells expressing WT αIIbβ3 and the L974N mutant were resuspended (11). By contrast, FAK phosphorylation was unchanged when the G972N cells were resuspended, implying that the G972N mutation promotes downstream signaling events known to depend on integrin clustering. Taken together, the results shown in Figs. 1 and 2 demonstrate that replacing G972 in the αIIb TM helix with Asn shifts αIIbβ3 from its inactive to its active conformation and induces the formation of αIIbβ3 clusters as well.

Mutations That Disrupt αIIb TM Domain Dimerization Increase αIIbβ3 Activity. G972 is the first residue of a GxxxG motif that is essential for αIIb TM helix oligomerization (7). We used the TOXCAT assay to assess the effect of G972N on the dimerization of the αIIb TM helix. TOXCAT measures the dimerization of a chimeric protein containing a TM helix in the *E. coli* inner membrane via the transcriptional activation of the reporter gene CAT (17). We found that replacing G972 with Asn resulted in a 55% decrease in CAT expression compared with the WT αIIb TM helix, whereas L974N, a mutation that has no effect on αIIbβ3 function, resulted in CAT expression that was similar to WT αIIb (Fig. 3*A*). The disruptive effect of G972N on αIIb TM helix dimerization in bacterial membranes was confirmed by equilibrium sedimentation in dodecylphosphocholine micelles: introducing the mutation into a peptide encompassing the αIIb TM and CYT domains resulted in an ≈3-fold decrease in its tendency to oligomerize (Table 2). By contrast, mutating G708

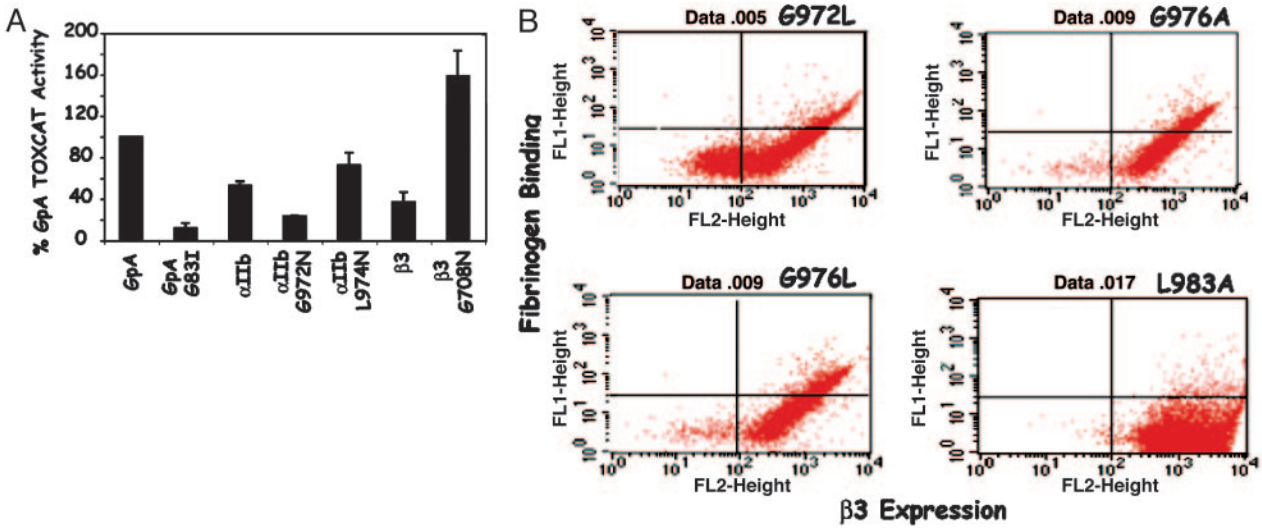

Fig. 3. Effect of mutations that disrupt αIIb TM domain dimerization on αIIbβ3 function. (*A*) Measurement of TM helix association using the TOXCAT assay. CAT expression induced by chimeric proteins containing the indicated αIIb and β3 TM helices was determined by CAT-ELISA and was compared to that induced by chimeric proteins containing the GpA-WT helix and the poorly dimerizing GpA mutant G83I. Data shown are the mean and 1 SE of four to six experiments. (*B*) Dot plots of fibrinogen and anti-β3 mouse mAb SSA6 binding to cells expressing the disruptive αIIb TM domain mutants G972N, G976L, and G976A and the permissive mutation L983A. FITC fluorescence, representing fibrinogen binding, is shown on the *y* axis, and PE fluorescence, representing β3 expression, is shown on the *x* axis.

to Asn within the β3 TM helix (Table 1) resulted in an 8-fold increase in the tendency of a β3 TM/CYT peptide to oligomerize. These data imply that the αIIbβ3 activation and clustering induced by G972N in the αIIb TM domain is not a result of an enhancement in its ability to form homooligomers.

To confirm further this conclusion in eukaryotic cell membranes, we examined a series of mutations with impaired abilities to form αIIb homodimers. Mutating either Gly in the αIIb GxxxG motif to Ala, Leu, Val, or Ile impaired dimerization of the αIIb helix in TOXCAT (7). Therefore, we introduced the disruptive αIIb mutations G972L, G976A, and G976L, as well as the neutral mutation L983A, into WT αIIbβ3 and measured their effect on αIIbβ3 activity in CHO cells. As shown in Figs. 3*B* and 4, each of the disruptive mutations induced constitutive fibrinogen binding to αIIbβ3, as well as αIIbβ3 clustering, whereas the neutral L983A mutation did neither. Thus, these experiments confirm that disruptive mutations in the αIIb GxxxG motif not only impair homodimerization of the αIIb TM helix *in vivo* but also shift αIIbβ3 to its active conformation.

L980A, a Mutation in the αIIb TM Domain Mutation That Enhances Its Dimerization, Induces Constitutive αIIbβ3 Activation. Unlike G972N, mutating L980 to Ala results in a 2.5-fold increase in CAT expression over the WT αIIb TM domain in TOXCAT, and its enhancing effect on αIIb TM helix oligomerization is apparent using SDS/PAGE and analytical ultracentrifugation (7). To determine whether the enhancing effect of L980A affects αIIbβ3 function, we introduced the mutation into full-length αIIb and compared fibrinogen binding to WT αIIbβ3 and the αIIb mutant. As shown in Fig. 5*A*, αIIbβ3 containing L980A constitutively binds ≈6.5-fold more fibrinogen than WT αIIbβ3 and ≈34% of the cells containing the mutant express constitutively activated αIIbβ3. Moreover, like other activating TM helix mutations, L980A caused αIIbβ3 patching on the CHO cell surface, consistent with αIIbβ3 clustering (Fig. 5*B*).

Structural Model of an αIIb/β3 TM Domain Heterodimer. Although isolated αIIb TM domains undergo homomeric association in micelles (5) and lipid bilayers (6), the ability of mutations that disrupt this association to activate αIIbβ3 implies that other interactions involving this domain must be involved in this process. Recently, Schneider and Engelman (6), using the GALLEX assay, reported that the αIIb and β3 TM domains undergo both homomeric and heteromeric associations in bacterial membranes, and Luo *et al.* (25) used disulfide bond-scanning of the αIIb and β3 TM domains to identify a heterodimerization

Table 2. Analytical ultracentrifugation of WT and mutant αIIb and β3 TM/CYT proteins

αIIb	$(P/L)_{50}$*	β3	$(P/L)_{50}$
WT	1.48×10^{-3}	WT	2.25×10^{-2}
G972N	4.68×10^{-3}	G708N	2.78×10^{-3}

*$(P/L)_{50}$ corresponds to the protein/detergent ratio at which the fraction of monomeric protein is 50% and is a measure of its tendency to oligomerize.

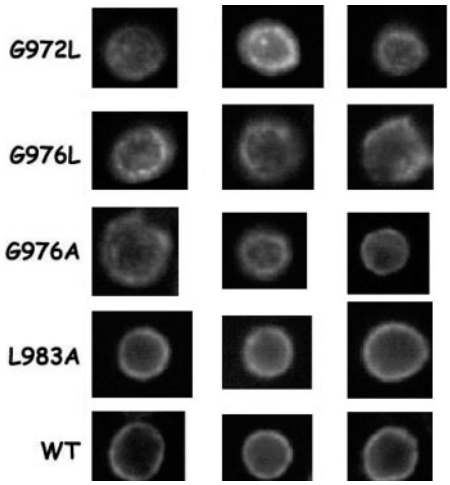

Fig. 4. Fluorescence microscopy of CHO cells expressing WT αIIbβ3 and the αIIb mutants G972L, G976L, G976A, and L983A. Cells were fixed with paraformaldehyde, incubated sequentially with the mAb SSA6 and FITC-labeled anti-mouse IgG, and examined by fluorescence microscopy. Representative images are shown.

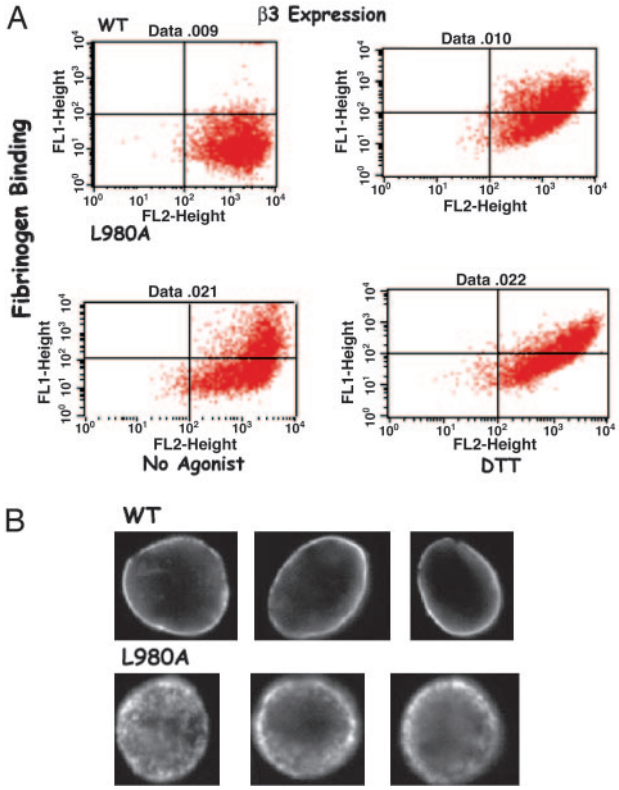

Fig. 5. An L980A mutation in the αIIb TM domain induces constitutive αIIbβ3 activity. (*A*) Dot plots of fibrinogen and anti-β3 mouse mAb SSA6 binding to cells expressing WT human αIIbβ3 and the enhancing αIIb TM domain mutant L980A. FITC fluorescence, representing fibrinogen binding is shown on the *y* axis, and PE fluorescence, representing β3 expression, is shown on the *x* axis. Fibrinogen binding was measured in the absence or presence of 5 mM DTT. (*B*) Fluorescence microscopy of CHO cells expressing WT αIIbβ3 and the αIIb L980A mutant. Cells were fixed, incubated with the mAb SSA6 and FITC-labeled anti-mouse IgG, and examined by fluorescence microscopy. Representative images are shown.

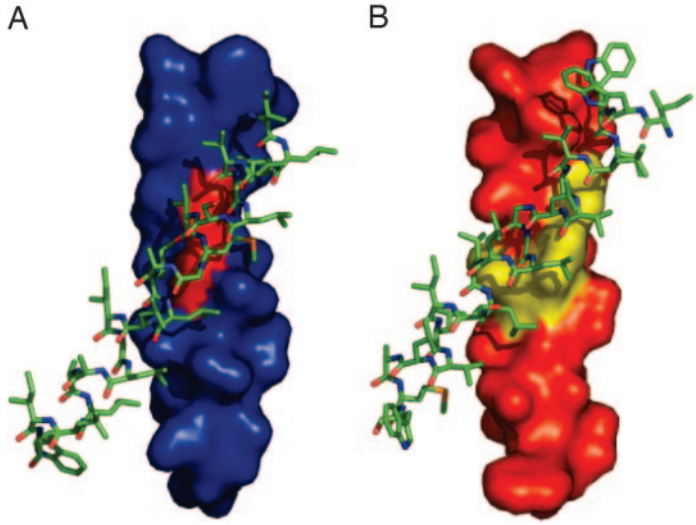

Fig. 6. Structural model of an αIIb/β3 TM domain heterodimer. Shown are space-filling models of the αIIb (*A*) and β3 (*B*) TM helices with the interfacial αIIb glycines 972 and 976 highlighted in red and interfacial β3 residues Val-700, Ile-704, and Leu-705 highlighted in yellow.

interface in the inactive integrin. Thus, these observations suggest that the αIIb GxxxG motif may participate in heteromeric interactions with the β3 subunit, and this interaction helps to maintain αIIbβ3 in an inactive state. To explore this possibility, we constructed an atomic model for an αIIb/β3 TM heterodimer. Structural fitness of the model was evaluated by using a recently devised scoring protocol that automatically incorporates mutagenesis data into the energy function. Initial docking attempts identified local minima with right- and left-handed crossing angles. The left-handed structures failed to converge to a single geometry, and none of the glycines in the αIIb GxxxG motif formed Cα–H hydrogen bonds with β3 carbonyls or side chains. Although these structures represent possible geometries for the heterodimeric interface (26, 27), we place more confidence in the right-handed structures, which show lower energies and more extensive interactions. The structures with the lowest energy had a GpA-like crossing angle of 15–40° (Figs. 6 *A* and *B*). In the structure with a 40° angle, αIIb Gly-972 and Gly-976 are involved in intimate contact with the β3 TM domain, explaining the sensitivity of the heterodimeric interface to mutation. Furthermore, although this model was made before the availability of disulfide crosslinking data from Luo *et al.* (25), there is good agreement over the faces of both the β3 and αIIb helices that contact in the complex.

Discussion

Integrin TM domains undergo homomeric and heteromeric interactions (6), but it has only recently become clear that these interactions may play an important role in regulating integrin function. Previously, we scanned the β3 TM domain with Asn residues and found that an appropriately placed Asn not only enhanced its homomeric association but also induced constitutive αIIbβ3 activity (11). Here, we studied the effect of αIIb TM domain mutations on aIIbβ3 function using Asn scanning mutagenesis, as well as mutations shown previously to disrupt or enhance the homomeric association of the αIIb TM domain (7). As was the case for β3, we found that an enhancing mutation, L980A, induced constitutive αIIbβ3 activity. This finding is consistent with the overall conclusions of our earlier studies. However, because L980A is close to the heterodimeric TM interface predicted in the current work, we cannot rule out the possibility that the disruption of this heterodimeric association could contribute to the ability of L980A to activate αIIbβ3.

We also found that a series of mutations that disrupt the GxxxG motif mediating homodimerization of the αIIb TM domain activate αIIbβ3 (7). The most likely explanation for this finding is that the GxxxG motif is involved not only in homomeric αIIb interactions but in heteromeric αIIb/β3 interactions as well. This conclusion is consistent with the findings of Schneider and Engelman (6), who used the GALLEX assay to demonstrate heteromeric, as well as homomeric, association of various integrin TM domains in bacterial membranes. Moreover, they found that mutations of the SxxxG motif in α4 and the GxxxG motif in β7 impaired the formation of α4 and β7 homodimers, as well as α4β7 heterodimers, suggesting that such motifs are important for both types of interaction.

Using a cysteine-scanning approach to capture a αIIb/β3 TM domain heterodimer and localize a heterodimerization interface, Luo *et al.* (25) observed the formation of disulfide bonds between cysteine substitutions in the αIIb and β3 TM domains with a helical periodicity and involving residues at positions 966, 968, 969, 971, and 972 in αIIb and 693, 694, 696, 697, 698, and 700 in β3, implying there is a unique orientation between the two helices. Our own computational protocol, which explicitly considers data from the αIIb/β3 TM mutagenesis experiments, predicted a helix–helix interface that is in good agreement with these mutagenesis data. Although the data are not yet sufficient to provide a single model, some features are clearly predicted and are different from previous models. Structures with a GpA-like crossing angle of 15–40° had the lowest overall energy;

other structures consistent with the data had the same sides of the helices in the interface, but the helical axes crossed at different angles. Consistent with results reported by Luo *et al.* (25), the model places αIIb G972 and β3 L697 in the heterodimer interface, but unlike previous models, it places the β3 SxxxA motif on the opposite face of the helix. It is also noteworthy that a GpA-like crossing angle predicts αIIb and β3 TM domains of 26–27 residues, placing the first several residues of what has been considered to be their CYT domains (28) in the membrane bilayer, a prediction consistent with the borders of integrin TM domains determined by glycosylation mapping (29, 30).

Models of αIIb/β3 TM helix heterodimers have been reported previously. Gottschalk and coworkers (26) docked 16 integrin heterodimer pairs, including αIIbβ3, by using a simulated annealing algorithm and five variable parameters. Based on sequence alignment and prior analysis of the GxxxG motif, they identified a GpA-like structure containing the αIIb GxxxG and β3 SxxxA motifs, as well as a second conformation in which the β-subunit is rotated by ≈100°. Subsequent annealing and molecular dynamics simulations supported a model in which the αIIb and β3 TM domains interact weakly in a right-handed coiled-coil when the integrin is in the low-affinity conformation (27). Adair and Yeager (31) also proposed that the αIIb and β3 TM domains associate in an α-helical coiled coil. The αIIb/β3 sequence was aligned by using the putative Arg-Asp clasp (2) and mapped onto a left-handed leucine zipper or a right-handed coiled coil.

Taken together with previous work, our data suggest a push–pull mechanism for integrin activation. Any process that destabilizes the association of the α and β TM domains would be expected to allow dissociation of the TM domains with concomitant activation of the integrin. Thus, mutations that disrupt the heteromeric TM helix interface activate αIIbβ3. Furthermore, the CYT domains are also believed to interact with one another, and they may play important roles in integrin activation. Mutations or modifications that disrupt the interaction of the α with the β CYT domains should weaken the interactions of the proximal TM domains, thereby leading to activation.

Conversely, any intermolecular interaction that either requires the separation of the α and β TM/CYT domains or is more favorable when they dissociate should pull the equilibrium toward the activated state. Thus, interaction of the cytoplasmic domains with talin or other cytoplasmic proteins would lead to activation if complex formation weakened the interactions between the α and β TM/CYT domains. Previously, we hypothesized that homooligomerization of the TM domains can also drive the equilibrium toward the activated state. Our results with mutations to the TM domain of β3 and the homooligomerization-promoting mutation L980A are consistent with this hypothesis. Nonetheless, our results with mutations that disrupt the homomeric interaction of the αIIb TM domain, but activate αIIbβ3, indicate that homooligomerization is not essential for activation. Instead, homooligomerization appears to be one of several mechanisms to pull the equilibrium toward the activated state.

We thank Dr. Donald Engelman for kindly providing the TOXCAT plasmids. This work was supported by National Institutes of Health Grants HL40387 and HL54500.

1. Kim, M., Carman, C. V. & Springer, T. A. (2003) *Science* **301,** 1720–1725.
2. Vinogradova, O., Velyvis, A., Velyviene, A., Hu, B., Haas, T., Plow, E. & Qin, J. (2002) *Cell* **110,** 587–597.
3. Tadokoro, S., Shattil, S. J., Eto, K., Tai, V., Liddington, R. C., de Pereda, J. M., Ginsberg, M. H. & Calderwood, D. A. (2003) *Science* **302,** 103–106.
4. Takagi, J., Petre, B., Walz, T. & Springer, T. (2002) *Cell* **110,** 599–611.
5. Li, R., Babu, C. R., Lear, J. D., Wand, A. J., Bennett, J. S. & DeGrado, W. F. (2001) *Proc. Natl. Acad. Sci. USA* **98,** 12462–12467.
6. Schneider, D. & Engelman, D. M. (2004) *J. Biol. Chem.* **279,** 9840–9846.
7. Li, R., Gorelik, R., Nanda, V., Law, P. B., Lear, J. D., DeGrado, W. F. & Bennett, J. S. (2004) *J. Biol. Chem.* **279,** 26666–26673.
8. Gottschalk, K. E. & Kessler, H. (2004) *Structure (Cambridge, MA)* **12,** 1109–1116.
9. Choma, C., Gratkowski, H., Lear, J. D. & DeGrado, W. F. (2000) *Nat. Struct. Biol* **7,** 161–166.
10. Zhou, F. X., Cocco, M. J., Russ, W. P., Brunger, A. T. & Engelman, D. M. (2000) *Nat. Struct. Biol.* **7,** 154–160.
11. Li, R., Mitra, N., Gratkowski, H., Vilaire, G., Litvinov, R., Nagasami, C., Weisel, J. W., Lear, J. D., DeGrado, W. F. & Bennett, J. S. (2003) *Science* **300,** 795–798.
12. Russ, W. P. & Engelman, D. M. (2000) *J. Mol. Biol.* **296,** 911–919.
13. Weisel, J. W., Nagaswami, C., Vilaire, G. & Bennett, J. S. (1992) *J. Biol. Chem.* **267,** 16637–16643.
14. Basani, R. B., D'Andrea, G., Mitra, N., Vilaire, G., Richberg, M., Kowalska, M. A., Bennett, J. S. & Poncz, M. (2001) *J. Biol. Chem.* **276,** 13975–13981.
15. Hato, T., Pampori, N. & Shattil, S. J. (1998) *J. Cell. Biol.* **141,** 1685–1695.
16. Pace, C. N., Vajdos, F., Fee, L., Grimsley, G. & Gray, T. (1995) *Protein Sci.* **4,** 2411–2423.
17. Russ, W. P. & Engelman, D. M. (1999) *Proc. Natl. Acad. Sci. USA* **96,** 863–868.
18. Bower, M. J., Cohen, F. E. & Dunbrack, R. L., Jr. (1997) *J. Mol. Biol.* **267,** 1268–1282.
19. Ponder, J. W. & Case, D. A. (2003) *Adv. Protein Chem.* **66,** 27–85.
20. Lear, J. D., Gratkowski, H. & DeGrado, W. F. (2001) *Biochem. Soc. Trans.* **29,** 559–564.
21. Fleming, K. G., Ren, C. C., Doura, A. K., Eisley, M. E., Kobus, F. J. & Stanley, A. M. (2004) *Biophys. Chem.* **108,** 43–49.
22. Dawson, J. P., Melnyk, R. A., Deber, C. M. & Engelman, D. M. (2003) *J. Mol. Biol.* **331,** 255–262.
23. Parsons, J. T. (2003) *J. Cell. Sci.* **116,** 1409–1416.
24. Arias-Salgado, E. G., Lizano, S., Sarkar, S., Brugge, J. S., Ginsberg, M. H. & Shattil, S. J. (2003) *Proc. Natl. Acad. Sci. USA* **100,** 13298–13302.
25. Luo, B. H., Springer, T. A. & Takagi, J. (2004) *PLoS Biol.* **2,** 776–786.
26. Gottschalk, K. E., Adams, P. D., Brunger, A. T. & Kessler, H. (2002) *Protein Sci.* **11,** 1800–1812.
27. Gottschalk, K. E. & Kessler, H. (2004) *FEBS Lett.* **557,** 253–258.
28. Hughes, P. E., Diaz-Gonzales, F., Leong, L., Wu, C., McDonald, J. A., Shattil, S. J. & Ginsberg, M. H. (1996) *J. Biol. Chem.* **271,** 6571–6574.
29. Armulik, A., Nilsson, I., von Heijne, G. & Johansson, S. (1999) *J. Biol. Chem.* **274,** 37030–37034.
30. Stefansson, A., Armulik, A., Nilsson, I., von Heijne, G. & Johansson, S. (2004) *J. Biol. Chem.* **279,** 21200–21205.
31. Adair, B. D. & Yeager, M. (2002) *Proc. Natl. Acad. Sci. USA* **99,** 14059–14064.